2008 American Control Conference
Westin Seattle Hotel, Seattle, Washington, USA
June 11-13, 2008

Spherical Simplex Sigma-Point Kalman Filters: A comparison in the inertial navigation of a terrestrial vehicle

Juan G. Castrejón Lozano, Luis R. Garca Carrillo, Alejandro Dzul and Rogelio Lozano

***Abstract*— To determine the position of a mobile robot continues being a complex and interesting challenge in localization algorithms, whose solution requires the use of estimation techniques of nonlinear systems, a well selection of sensors that fulfill the restrictions imposed by the characteristics of the system, and the selection of the suitable algorithm of navigation. In this article, the performance of three variants of Sigma Point Kalman Filter (SPKF) are analyzed and compared, where the selection strategy of spherical simplex sigma points is used in order to improve its performance for real time execution. The analyzed filters are applied to an inertial navigation system that is used for the localization of a terrestrial mobile vehicle. The obtained results of the comparative analysis are illustrated by some simulations.**

Key words: Kalman filters, mobile robots, estimation algorithms, inertial navigation, estimation of position.

I. Introduction

Localization represents one of the more critic abilities for an autonomous mobile robot [9]. An autonomous mobile robot must use the relative and absolute measurements provided by its sensors in order to estimate its own position. However, the natural uncertainty of the sensor measurements and the possible errors in the navigation model, make necessary the use of all available information in order to obtain an optimal data fusion. Lamentably, the theories and techniques that make reality this objective still follow in development, existing a great amount of challenges in the theoretical and technological fields. In the first field, an optimal solution that can be implemented to estimate nonlinear systems does not exist, then this leads to research on approximate solutions [14]. In the second field, in spite of the continuous improvements in miniaturization and performance of the useful sensors in the localization problem, its cost/performance–size relation remains much smaller than desirable [12].

Some of the solutions more recently proposed, about nonlinear system estimation, are the Sigma Point Kalman Filters (SPKF), which have been developed in order to surpass the limitations displayed by the widely used Extended Kalman Filter (EKF) [3]. Nevertheless, in spite of the undeniable advantages over the EKF, the SPKF have a relatively poor performance concerning the run time execution, due to the high computational cost that entails to propagate each sigma point by the nonlinear transformation. This has motivated the search of other solutions like the use of SPKF additive versions, which have the disadvantage of loss of exactitude and a greater difficulty of tuning. Since the reduction of the number of sigma points represents a main aspect, in order to decrease the run time execution, an alternate criterion of point selection has been developed recently [7], it is called as Spherical Simplex Sigma Points. This criterion allows for a system of dimension n, to make a selection of $n+2$ sigma points, instead of the well-known amount of $2n+1$. We use this criterion in order to analyse their behaviors in a navigation task.

In the present article, the performance of three variants of the SPKF, applied to the inertial navigation of a terrestrial vehicle is analyzed in simulation. These variants use the selection criterion of spherical simplex sigma points. In section II, the theoretical methodology of the SPKF, as well as the reason for their different variants, is reviewed. In Section III, the model of inertial navigation aided with DGPS measurements, used in the terrestrial vehicle is presented. Later, in section IV, the kinematic model used in simulation is introduced. In section V, the results obtained by simulations are showed. Finally, the conclusions are given in section VI.

II. Sigma Point Kalman Filters

The Unscented Kalman Filter (UKF) is the more known member of a family of Kalman filters, known as Sigma Point Kalman Filters [2], [4]. The variants that have been developed for this filter are intended to improve its performance in several areas. The additive UKF was set out in order to reduce the number of mathematical calculations performed in each iteration, without using the augmented states of the traditional UKF. This reduces significantly the computational load of the filter that is mainly used in the calculation and propagation of the sigma points, and makes it more appropriate to be executed in real-time systems. The square root UKF was developed to prevent numerical instabilities to which the algorithm is exposed, being necessary to conserve the covariance matrix of the state errors as semidefined positive [13]. In addition to the numerical robustness reached, a reduction in computational cost is obtained. These three filters are described below in their spherical simplex form.

This work was partially supported by CONACYT, LAFMAA and DGEST

Juan G. Castrejón Lozano, Luis R. Garca Carrillo and Alejandro Dzul are with the División de Estudios de Posgrado e Investigación of the Instituto Tecnológico de la Laguna, Blvd. Revolución y Cuauhtémoc, 27000 Torreón, Coahuila, Mexico {jcastrejon, dzul}@faraday.itlalaguna.edu.mx

Rogelio Lozano is with the Heudiasyc UMR-CNRS 6599, Université de Technology de Compiègne, Centre de Recherches de Royallieu, 60200 Compiègne, France rlozano@hds.utc.fr

A. Standard UKF Algorithm

The standard UKF algorithm is applied to nonlinear discret time systems described by the equations [5]:

$$\boldsymbol{x}_k = \boldsymbol{f}(\boldsymbol{x}_{k-1}, \boldsymbol{w}_{k-1}) \quad (1)$$

$$\boldsymbol{y}_k = \boldsymbol{h}(\boldsymbol{x}_k, \boldsymbol{v}_k) \quad (2)$$

where $\boldsymbol{x}_k \in \mathbb{R}^n$ is the state vector, $\boldsymbol{y}_k \in \mathbb{R}^m$ is the measurement vector, $\boldsymbol{f}(\cdot)$ is a nonlinear function of the state propagation, $\boldsymbol{h}(\cdot)$ is a nonlinear function of measurements, $\boldsymbol{w}_k \in \mathbb{R}^n$ and $\boldsymbol{v}_k \in \mathbb{R}^m$ are the process and measurement noise whose covariances are given by $Q_k \in \mathbb{R}^{n\times n}$ and $R_k \in \mathbb{R}^{m\times m}$ respectively.

The UKF uses a vector of augmented states defined by

$$\boldsymbol{x}_k^a = \begin{bmatrix} \boldsymbol{x}_k \\ \boldsymbol{w}_k \\ \boldsymbol{v}_k \end{bmatrix} \in \mathbb{R}^{2n+m} \quad (3)$$

whose augmented matrix of covariance, is given by

$$P^a = \begin{bmatrix} P_{x_k} & \mathbf{0} & \mathbf{0} \\ \mathbf{0} & Q_k & \mathbf{0} \\ \mathbf{0} & \mathbf{0} & R_k \end{bmatrix} \in \mathbb{R}^{(2n+m)\times(2n+m)} \quad (4)$$

where P_x is the covariance matrix of the estimation error.

First, a set of sigma points is calculated applying the equation:

$$\mathcal{X}_{k-1}^a = \left[\hat{\boldsymbol{x}}_{k-1}^a \quad \hat{\boldsymbol{x}}_{k-1}^a + \gamma\sqrt{P_{k-1}^a} \quad \hat{\boldsymbol{x}}_{k-1}^a - \gamma\sqrt{P_{k-1}^a}\right] \quad (5)$$

where $\mathcal{X}_{k-1}^a \in \mathbb{R}^{L\times(2L+1)}$ is the sigma points matrix, being $L = 2n+m$. The parameter $\gamma = \sqrt{L+\rho}$ being $\rho = \alpha^2(L+\kappa) - L$. The constant α determines the sigma points spread and it is often a positive small value ($1\times 10^{-4} \leq \alpha \leq 1$). The scalar $\kappa \geq 0$ is a parameter that guarantees positive semidefiniteness of the covariance matrix, a good value for this parameter is $\kappa = 0$.

Next, a transformed set of sigma points is evaluated for each i-th column of the matrix $\mathcal{X}$, by means of the nonlinear function of the system:

$$\mathcal{X}_{k|i} = \boldsymbol{f}(\mathcal{X}_{k-1|i}^x, \mathcal{X}_{k-1|i}^w), \qquad i = 0, \ldots, 2L \quad (6)$$

At the prediction stage, the means and error covariances of the states and measurements are calculated as

$$\hat{\boldsymbol{x}}_k^- = \sum_{i=0}^{2L} w_i^m \mathcal{X}_{k|i} \quad (7)$$

$$P_{x_k}^- = \sum_{i=0}^{2L} w_i^c [\mathcal{X}_{k|i} - \hat{\boldsymbol{x}}_k^-][\mathcal{X}_{k|i} - \hat{\boldsymbol{x}}_k^-]^T \quad (8)$$

$$\mathcal{Y}_{k|i} = \boldsymbol{h}(\mathcal{X}_{k|i}, \mathcal{X}_{k-1|i}^v), \qquad i = 0, \ldots, 2L \quad (9)$$

$$\hat{\boldsymbol{y}}_k^- = \sum_{i=0}^{2L} w_i^m \mathcal{Y}_{k|i} \quad (10)$$

$$P_{y_k} = \sum_{i=0}^{2L} w_i^c [\mathcal{Y}_{k|i} - \hat{\boldsymbol{y}}_k^-][\mathcal{Y}_{k|i} - \hat{\boldsymbol{y}}_k^-]^T \quad (11)$$

$$P_{xy_k} = \sum_{i=0}^{2L} w_i^c [\mathcal{X}_{k|i} - \hat{\boldsymbol{x}}_k^-][\mathcal{Y}_{k|i} - \hat{\boldsymbol{y}}_k^-]^T \quad (12)$$

For the correction stage, the following equations are used:

$$K_k = P_{xy_k} P_{y_k}^{-1} \quad (13)$$

$$\hat{\boldsymbol{x}}_k = \hat{\boldsymbol{x}}_k^- + K_k(\boldsymbol{y}_k - \hat{\boldsymbol{y}}_k^-) \quad (14)$$

$$P_{x_k} = P_{x_k}^- - K_k P_{y_k} K_k^T \quad (15)$$

B. Spherical Simplex Sigma Point Approach

The selection criterion of spherical simplex sigma points is a new and better selection strategy for the Unscented Transformation (UT) [7], which significantly allows to reduce the number of sigma points propagated, and by this fact, the implementation of filters becomes more suitable for real-time systems, where the limitations of computational cost are extremely restrictive. This selection strategy defines a minimum set of points located in a hyper-sphere. For a n-dimensional space, only $n+2$ points are required. The points are in a radius that is proportional to $\sqrt{n}$, and the weight applied to each point is proportional to $1/n$.

Consider a random variable $\boldsymbol{x} \in \mathbb{R}^n$ that is propagated through an arbitrary nonlinear function $\boldsymbol{y} = \boldsymbol{g}(\boldsymbol{x})$, being $\boldsymbol{y} \in \mathbb{R}^m$ and $n,\ m \in \mathbb{N}_+$. Assume that $\boldsymbol{x}$ has mean $\hat{\boldsymbol{x}}$ and covariance P_x. In order to calculate the statistics of $\boldsymbol{y}$ (mean and covariance), a set of $n+2$ sigma points is formed $\{\mathcal{X}_i; i = 0, \ldots, n+1\}$, where $\mathcal{X}_i \in \mathbb{R}^n$. The sigma points are calculated using the following criterion

$$\mathcal{X}_i = \bar{\boldsymbol{x}} + \sqrt{P_x}\mathcal{Z}_i \qquad i = 0, \ldots, n+1 \quad (16)$$

where $\sqrt{P_x}$ indicates the square root of the covariance matrix P_x, and $\mathcal{Z}_i$ is i-th column of the spherical simplex sigma point matrix, previously calculated by the following algorithm

1) Choose the value $0 \leq W_0 \leq 1$
2) The sequence of weights is chosen as

$$W_i = (1 - W_0)/(n+1) \quad (17)$$

3) In order to use the advantages of the scaled transformation, the previous weights are transformed by the following way [6]:

$$w_i = \begin{cases} 1 + (W_0 - 1)/\alpha^2 & i = 0 \\ W_i/\alpha^2 & i \neq 0 \end{cases} \quad (18)$$

where α is the sigma points scalar factor ($0 \leq \alpha \leq 1$), which allows to minimize the higher order errors.

4) The vector sequence is initialized as

$$\mathcal{Z}_0^1 = [0],\ \mathcal{Z}_1^1 = \left[-\frac{1}{\sqrt{2w_1}}\right] \text{ y } \mathcal{Z}_2^1 = \left[\frac{1}{\sqrt{2w_1}}\right] \quad (19)$$

5) The vector sequence is expanded for $j = 2, \ldots, n$ according to

$$\mathcal{Z}_i^j = \begin{cases} \begin{bmatrix} \mathcal{Z}_0^{j-1} \\ 0 \end{bmatrix} & \text{for } i = 0 \\[2ex] \begin{bmatrix} \mathcal{Z}_i^{j-1} \\ -\frac{1}{\sqrt{j(j+1)w_1}} \end{bmatrix} & \text{for } i = 1, \ldots, j \\[2ex] \begin{bmatrix} \mathbf{0}_{j-1} \\ \frac{j}{\sqrt{j(j+1)w_1}} \end{bmatrix} & \text{for } i = j+1 \end{cases} \quad (20)$$

6) Finally, in order to incorporate information of higher order, define [8]:

$$\begin{array}{ll} w_0^m = w_0 & i=0 \\ w_0^c = w_0 + (1-\alpha^2+\beta) & i=0 \\ w_i^m = w_i^c = w_i & i = 1\ldots,n+2 \end{array} \tag{21}$$

where β denotes a parameter that affects the weight of the zeroth sigma point for the calculation of the covariance, allowing to minimize higher order errors if a previous knowledge of the distribution is provided for $\boldsymbol{x}$. For a Gaussian distribution, the optimal selection is $\beta = 2$.

Once the sigma points have been calculated in the previous form, it is necessary to propagate them through the next nonlinear function

$$\mathcal{Y}_i = \boldsymbol{g}(\mathcal{X}_i) \qquad i = 0,\ldots,n+1 \tag{22}$$

The mean and covariance of $\boldsymbol{y}$ are approximated using a mean and covariance of weighted samples of the transformed sigma points in the following way

$$\bar{\boldsymbol{y}} \approx \sum_{i=0}^{n+1} w_i^m \mathcal{Y}_i \tag{23}$$

$$P_y \approx \sum_{i=0}^{n+1}\sum_{j=0}^{n+1} w_i^c \mathcal{Y}_i \mathcal{Y}_j^T \tag{24}$$

$$P_{xy} \approx \sum_{i=0}^{n+1}\sum_{j=0}^{n+1} w_i^c \mathcal{X}_i \mathcal{Y}_j^T \tag{25}$$

where w_i^m, w_i^c are the mean and covariance scalar weights, defined previously.

C. SS-UKF Algorithm

The SS-UKF algorithm is applied to nonlinear systems described by (1) and (2).

First, a set of sigma points is calculated applying the equation

$$\mathcal{X}_{k-1|i}^a = \hat{\boldsymbol{x}}_{k-1}^a + \sqrt{P_{k-1}^a}\mathcal{Z}_i \qquad i = 0,\ldots,L+1 \tag{26}$$

where $\mathcal{X}_{k-1}^a \in \mathbb{R}^{L\times(L+2)}$ is the sigma points matrix, being $L = 2n+m$.

Now, a transformed set of sigma points is evaluated for each i-th column of the $\mathcal{X}_k^a$ matrix, by means of the nonlinear function system

$$\mathcal{X}_{k|i} = \boldsymbol{f}(\mathcal{X}_{k-1|i}^x, \mathcal{X}_{k-1|i}^w), \qquad i = 0,\ldots,L+1 \tag{27}$$

At the prediction stage, the mean of the states is calculated as

$$\hat{\boldsymbol{x}}_k^- = \sum_{i=0}^{L+1} w_i^m \mathcal{X}_{k|i} \tag{28}$$

and the covariance prediction of the estimation error as

$$P_{x_k}^- = \sum_{i=0}^{L+1} w_i^c [\mathcal{X}_{k|i} - \hat{\boldsymbol{x}}_k^-][\mathcal{X}_{k|i} - \hat{\boldsymbol{x}}_k^-]^T \tag{29}$$

Next, the observation model is applied to each sigma points as follows

$$\mathcal{Y}_{k|i} = \boldsymbol{h}(\mathcal{X}_{k|i}, \mathcal{X}_{k-1|i}^v), \qquad i = 0,\ldots,L+1 \tag{30}$$

The prediction of the observation is calculated by means of the following equation

$$\hat{\boldsymbol{y}}_k^- = \sum_{i=0}^{L+1} w_i^m \mathcal{Y}_{k|i} \tag{31}$$

in addition, the output covariance is given by

$$P_{y_k} = \sum_{i=0}^{L+1} w_i^c [\mathcal{Y}_{k|i} - \hat{\boldsymbol{y}}_k^-][\mathcal{Y}_{k|i} - \hat{\boldsymbol{y}}_k^-]^T \tag{32}$$

The prediction stage finalizes with the calculation of the crossed correlation matrix, determined by

$$P_{xy_k} = \sum_{i=0}^{L+1} w_i^c [\mathcal{X}_{k|i} - \hat{\boldsymbol{x}}_k^-][\mathcal{Y}_{k|i} - \hat{\boldsymbol{y}}_k^-]^T \tag{33}$$

For the correction stage, the Kalman gain is calculated by

$$K_k = P_{xy_k} P_{y_k}^{-1} \tag{34}$$

Next, the corrected estimation of the state vector, is determined by means of

$$\hat{\boldsymbol{x}}_k = \hat{\boldsymbol{x}}_k^- + K_k(\boldsymbol{y}_k - \hat{\boldsymbol{y}}_k^-) \tag{35}$$

Finally, the covariance matrix correction of the estimation error, is calculated by the following equation

$$P_{x_k} = P_{x_k}^- - K_k P_{y_k} K_k^T \tag{36}$$

D. Additive SS-UKF Algorithm

The additive SS-UKF algorithm is applied to nonlinear systems described by the equations [2]:

$$\boldsymbol{x}_k = \boldsymbol{f}(\boldsymbol{x}_{k-1}) + \boldsymbol{w}_{k-1} \tag{37}$$

$$\boldsymbol{y}_k = \boldsymbol{h}(\boldsymbol{x}_k) + \boldsymbol{v}_k \tag{38}$$

where it is assumed that the process and measurement noises are additives. Next, we show the differences between the resulting algorithm with respect to the augmented SS-UKF.

The set of sigma points is calculated from the non-augmented states

$$\mathcal{X}_{k-1|i} = \hat{\boldsymbol{x}}_{k-1} + \sqrt{P_{x_{k-1}}}\mathcal{Z}_i, \qquad i = 0,\ldots,n+1 \tag{39}$$

where $\mathcal{X}_{k-1} \in \mathbb{R}^{n\times(n+2)}$, $\hat{\boldsymbol{x}}_{k-1} \in \mathbb{R}^n$ and $P_{x_{k-1}} \in \mathbb{R}^{n\times n}$.

The prediction equations are defined as

$$\mathcal{X}^*_{k|i} = \boldsymbol{f}(\mathcal{X}_{k-1|i}), \qquad i = 0, \ldots, n+1 \tag{40}$$

$$\hat{\boldsymbol{x}}^-_k = \sum_{i=0}^{n+1} w^m_i \mathcal{X}^*_{k|i} \tag{41}$$

$$P^-_{x_k} = \sum_{i=0}^{n+1} w^c_i [\mathcal{X}^*_{k|i} - \hat{\boldsymbol{x}}^-_k][\mathcal{X}^*_{k|i} - \hat{\boldsymbol{x}}^-_k]^T + Q_k \tag{42}$$

$$\mathcal{X}_k = [\mathcal{X}^*_k \quad \mathcal{X}^*_{k|0} + \sqrt{Q_k}\mathcal{Z}], \qquad n \to 2n \tag{43}$$

$$\mathcal{Y}_{k|i} = \boldsymbol{h}(\mathcal{X}_{k|i}), \qquad i = 0, \ldots, n+1 \tag{44}$$

$$\hat{\boldsymbol{y}}^-_k = \sum_{i=0}^{n+1} w^m_i \mathcal{Y}_{k|i} \tag{45}$$

$$P_{y_k} = \sum_{i=0}^{n+1} w^c_i [\mathcal{Y}_{k|i} - \hat{\boldsymbol{y}}^-_k][\mathcal{Y}_{k|i} - \hat{\boldsymbol{y}}^-_k]^T \tag{46}$$

Since the observation noise is independent and additive, now the covariance of innovation is given by

$$P_{v_k} = P_{y_k} + R_k \tag{47}$$

$$P_{xy_k} = \sum_{i=0}^{n+1} w^c_i [\mathcal{X}_{k|i} - \hat{\boldsymbol{x}}^-_k][\mathcal{Y}_{k|i} - \hat{\boldsymbol{y}}^-_k]^T \tag{48}$$

Finally, the correction stage is defined as follows

$$K_k = P_{xy_k} P^{-1}_{v_k} \tag{49}$$

$$\hat{\boldsymbol{x}}_k = \hat{\boldsymbol{x}}^-_k + K_k(\boldsymbol{y}_k - \hat{\boldsymbol{y}}^-_k) \tag{50}$$

$$P_{x_k} = P^-_{x_k} - K_k P_{v_k} K^T_k \tag{51}$$

E. Square Root SS-UKF Algorithm

This algorithm propagates and updates the square root of the covariance of the states directly in the form of Cholesky factor, using the sigma points approach and following three techniques of linear algebra for its theoretical development and implementation, which are: QR decomposition, Cholesky factor updating and efficient least squares based on pivoting.

The resulting algorithm can be resumed as

1) Calculate sigma points

$$\mathcal{X}^a_{k-1|i} = \hat{\boldsymbol{x}}^a_{k-1} + S^a_{k-1}\mathcal{Z}_i, \qquad i = 0, \ldots, L+1 \tag{52}$$

where

$$S^a_{k-1} = \begin{bmatrix} S_{x_{k-1}} & \mathbf{0} & \mathbf{0} \\ \mathbf{0} & S_w & \mathbf{0} \\ \mathbf{0} & \mathbf{0} & S_v \end{bmatrix} \tag{53}$$

and $S_x = \text{chol}\{P_x\}$, where $\text{chol}(\cdot)$ is a matrix function that performs the Cholesky factorization, $S_w = \sqrt{Q}$ and $S_v = \sqrt{R}$.

2) Time-update equations

$$\mathcal{X}_{k|i} = \boldsymbol{f}(\mathcal{X}^x_{k-1|i}, \mathcal{X}^w_{k-1|i}), \qquad i = 0, \ldots, L+1 \tag{54}$$

$$\hat{\boldsymbol{x}}^-_k = \sum_{i=0}^{L+1} w^m_i \mathcal{X}_{k|i} \tag{55}$$

$$S^-_{x_k} = \text{qr}\left\{\left[\sqrt{w^c_1}\left(\mathcal{X}_{k|1:L+1} - \hat{\boldsymbol{x}}^-_k\right)\right]\right\} \tag{56}$$

$$S^-_{x_k} = \text{cholupdate}\left(S^-_{x_k}, \mathcal{X}_{k|0} - \hat{\boldsymbol{x}}^-_k, w^c_0\right) \tag{57}$$

$$\mathcal{Y}_{k|i} = \boldsymbol{h}(\mathcal{X}_{k|i}, \mathcal{X}^v_{k-1|i}), \quad i = 0, \ldots, L+1 \tag{58}$$

$$\hat{\boldsymbol{y}}^-_k = \sum_{i=0}^{L+1} w^m_i \mathcal{Y}_{k|i} \tag{59}$$

where $\text{qr}(\cdot)$ is a function that carries out the QR decomposition, and $\text{cholupdate}(\cdot)$ is a function that performs the Cholesky factor updating.

3) Measurement-update equations

$$S_{y_k} = \text{qr}\left\{\left[\sqrt{w^c_1}\left(\mathcal{Y}_{k|1:L+1} - \hat{\boldsymbol{y}}^-_k\right)\right]\right\} \tag{60}$$

$$S_{y_k} = \text{cholupdate}\left\{S_{y_k}, \mathcal{Y}_{k|0} - \hat{\boldsymbol{y}}^-_k, w^c_0\right\} \tag{61}$$

$$P_{xy_k} = \sum_{i=0}^{L+1} w^c_i [\mathcal{X}_{k|i} - \hat{\boldsymbol{x}}^-_k][\mathcal{Y}_{k|i} - \hat{\boldsymbol{y}}^-_k]^T \tag{62}$$

$$K_k = (P_{xy_k} S^T_{y_k})/S_{y_k} \tag{63}$$

$$\hat{\boldsymbol{x}}_k = \hat{\boldsymbol{x}}^-_k + K_k(\boldsymbol{y}_k - \hat{\boldsymbol{y}}^-_k) \tag{64}$$

$$U = K_k S_{y_k} \tag{65}$$

$$S_{x_k} = \text{cholupdate}\left(S^-_{x_k}, U, -1\right) \tag{66}$$

III. Terrestrial Inertial Navigation

In order to obtain the navigation state vector related to a terrestrial vehicle, we take the next assumptions: consider that the vehicle moves only in the x–y plane, in a nonaccelerated and nonrotational frame (due to the relatively small displacement and the small time duration of the experiment), then we only require one gyroscope, which measure the angular rate in z, that is, the angular velocity of the yaw angle ψ, and also 2 accelerometers [10]. Previous assumptions result in the following equation

$$\begin{bmatrix} \dot{v}_x \\ \dot{v}_y \\ \dot{p}_x \\ \dot{p}_y \\ \dot{\psi} \\ \dot{a}_{xb} \\ \dot{a}_{yb} \\ \dot{\omega}_{zb} \end{bmatrix} = \begin{bmatrix} f^b_x \cos\psi + f^b_y \sin\psi \\ -f^b_x \sin\psi + f^b_y \cos\psi \\ v_x \\ v_y \\ \omega^b_z \\ 0 \\ 0 \\ 0 \end{bmatrix} \tag{67}$$

where v_x, v_y denote the x, y velocities in navigation coordinates; p_x, p_y represent the x, y positions. ψ is the Euler's angle in the z-axis; a_{xb}, a_{yb} and ω_{zb} represent the acceleration and gyro rate biases respectively. The gravity term has been omitted since the acceleration in the z-axis is not sensed.

The following IMU sensor model was used for both accelerometers and gyros [1]:

$$\tilde{a}(t) = a(t) + b(t) + \eta_v(t) \quad (68)$$
$$\dot{b} = \eta_u(t) \quad (69)$$

where $p(\eta_v) \cong N(0, \sigma_v)$ and $p(\eta_u) \cong N(0, \sigma_u)$ are zero-mean Gaussian random variables.

IV. Kinematic Model of a Terrestrial Vehicle

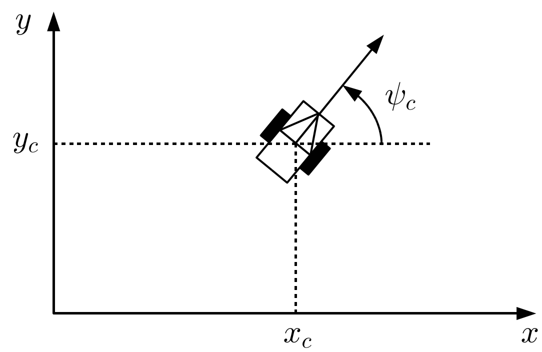

Fig. 1. Model of a car-like vehicle

The navigation algorithm is applied to a terrestrial mobile robot, for example a radio-controlled electrical car. The kinematics of this robot (Fig. 1) can be described by [11]:

$$\begin{bmatrix} \dot{x}_c \\ \dot{y}_c \\ \dot{\psi}_c \end{bmatrix} = \begin{bmatrix} v_c \cos\psi_c \\ v_c \sin\psi_c \\ \omega_c \end{bmatrix} \quad (70)$$

where x_c, y_c are the coordinates in the horizontal plane, and ψ_c is the angular displacement in z-axis (see Fig. 1). The control inputs v_c, and ω_c correspond respectively to the linear and angular rate of the vehicle.

V. Simulations

Using the kinematic model equations (70), the vehicle displacement has been simulated at a constant speed $v_c = 1$ m/s and a constant angular rate $\omega_c = 0.1$ rad/s, during a time of 25s. Both the DGPS and the inertial measurements were simulated. The noise implied in the inertial measurements has been modeled by additive Gaussian noise, as a random walk process. Additionally, the IMU quality has been degraded by increasing the additive noise variance and the measurement bias, and by reducing the IMU update rate. We consider that all the sensors measurements have been obtained at 10Hz. All the IMU variances (σ_u and σ_v) were artificially set to 3×10^{-1} for simplicity. In order to obtain the performance of each filter, 200 Monte Carlo simulations have been made. The results obtained are summarized in the table I, in which the square mean error (SME) of the states estimation x and y, and its variance are shown.

The trajectory executed by the vehicle is illustrated in Fig. 2, starting off from the origin $(0, 0)$, for $t_0 = 0$ s, and arriving at coordinates $(6, 18)$, for $t_n = 25$ s. In Fig. 3, the simulated DGPS measurements are represented. In Fig. 4 and 5, the position estimates of the coordinates x and y are showed separately in order to compare the different filters. Additional experiments, with a greater runtime (6 minutes), were simulated in order to validate the performance of these filters.

TABLE I

Comparison of SME of the mean and variance of the different filters

Algorithm	x (mean)	y (mean)	x (variance)	y (variance)
SSUKF	0.009748	0.012351	0.009170	0.006944
SRSSUKF	0.008070	0.010072	0.007442	0.004432
ASSUKF	0.010659	0.012770	0.010071	0.007406

A comparative analysis of the three filters was done, form which the following remarks can be concluded:

1) As the theory indicates, the augmented and square root Kalman filters show a better performance since they minimize the estimation error.
2) The additive SS-UKF provides a greater estimation error and it is more difficult to tune, this although the system is doubtlessly contaminated with additive Gaussian noise.
3) In spite of the previous results, the difference between the augmented and additive versions is not relatively so great, and on the other hand, the additive version is more suitable for systems that are executed in real-time, due to lower computational cost. Thus, the selection of the Kalman filter version, for the navigation algorithm, depends on the priorities that the platform require.

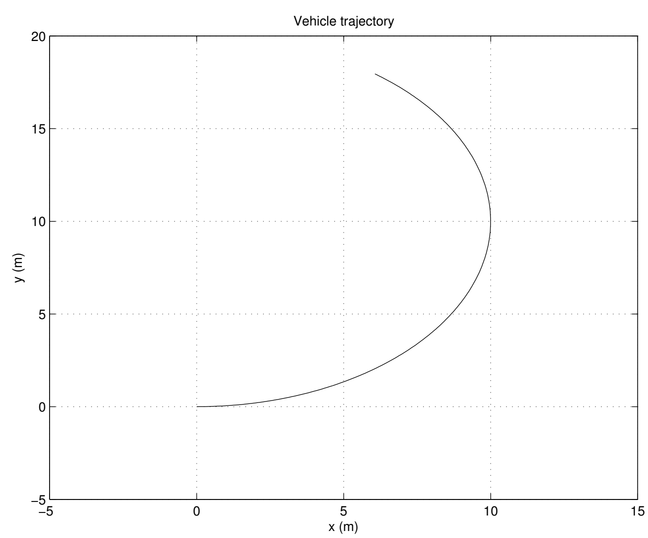

Fig. 2. Trajectory executed by the vehicle

VI. Conclusions

A comparative analysis of the standard, square root, and additive SS-UKF filters, which are part of the Sigma Point

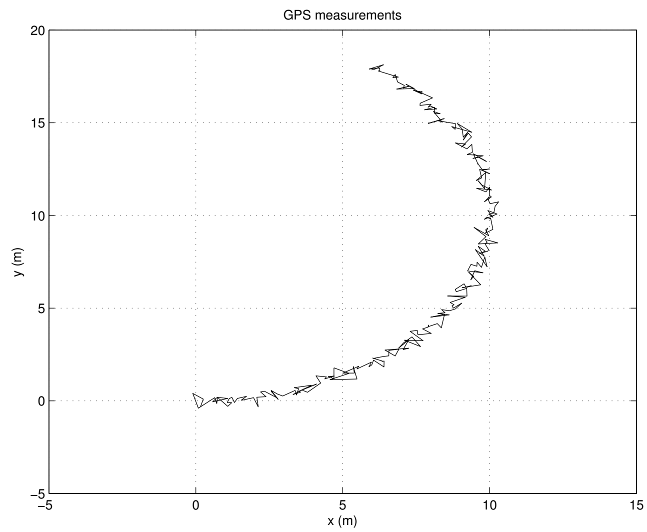

Fig. 3. Noised DGPS measurements obtained in simulation

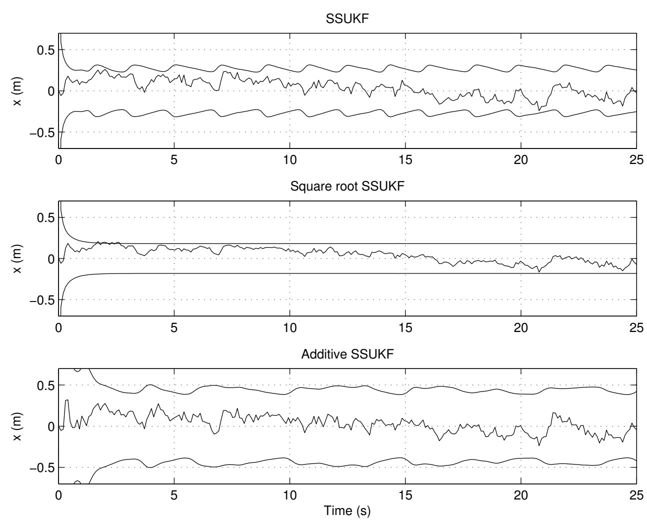

Fig. 4. Errors in x-position and 3σ bounds for each filter

Kalman Filters, was made. The analysis was based on the simulation of an inertial navigation system, in two dimensions, in order to estimate the position of a terrestrial vehicle, referred to the performance (in mean and variance) of the filters by means of Monte Carlo simulations. The obtained results showed that the additive SS-UKF is most advisable for real-time systems, due to its low computational cost, whereas if we desire a greater precision of the position estimation, then we will have to resort to the square root SS-UKF.

REFERENCES

[1] Crassidis, J.L., "Sigma-Point Kalman Filtering for Integrated GPS and Inertial Navigation", *in AIAA Guidance, Navigation, and Control Conference*, San Francisco, CA, USA, 2005.

[2] Simon Haykin, *Kalman Filtering and Neural Networks*, Wiley Inter-Science, 2001.

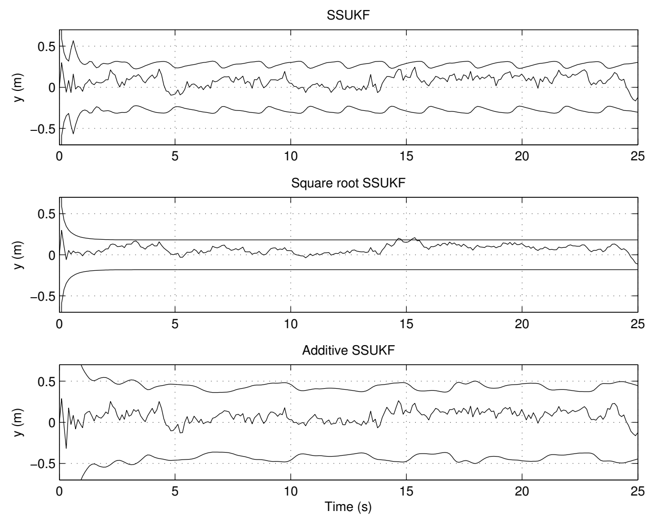

Fig. 5. Errors in y-position and 3σ bounds for each filter

[3] S. J. Julier, J. K. Uhlmann, and H. Durrant-Whyte. "A new approach for filtering nonlinear systems", *in Proceedings of the American Control Conference*, Seatle, USA, 1995.

[4] S. J. Julier, J. K. Uhlmann, and H. Durrant-Whyte, A New Approach for the Nonlinear Transformation of Means and Covariances in Linear Filters, *IEEE Transactions on Automatic Control*, Vol. 45, Issue 3, 1996.

[5] S. J. Julier, J. K. Uhlmann, "A New Extension of the Kalman Filter to Nonlinear Systems", *in Proceedings of the SPIE – Int. Soc. Opt. Eng.*, USA, 1997.

[6] S. J. Julier and J. K. Uhlmann, "The Scaled Unscented Transformation", *in Proceedings of the American Control Conference*, pp. 4555–4559, Anchorage, Alaska, USA, May 8-10, 2002.

[7] Simon J. Julier, "The Spherical Simplex Unscented Transformation", *in Proceedings of the American Control Conference*, Denver, Colorado, USA, June 4-6, 2003.

[8] S. J. Julier and J. K. Uhlmann, "Unscented Filtering and Nonlinear Estimation", *in Proceedings of the IEEE*, Vol. 92, No. 3, 2004.

[9] Rudy Negenborn, *Robot Localization and Kalman Filters*, Master Thesis, Utrecht University, Holland, 2003.

[10] R. M. Rogers and J. A. Schetz, *Applied Mathematics in Integrated Navigation Systems*, AIAA Education Series, Second edition, 2003.

[11] P. Soures, T. Hamel, V. Cadenat and A. Dzul, "A Reactive Path Following Controller for Mobile Robots", *in Proceedings of the IEEE Conference on Advances in Vehicle Control and Safety*, Amiens, France, 1998.

[12] D. Titterton and J. Weston, *Strapdown Inertial Navigation Technology*, Ed. Institution of Electrical Engineers, Second Edition, 2004.

[13] Rudolph van der Merwe and Eric Wan, "The Square–Root Unscented Kalman Filter for State and Parameter Estimation", *in Proceedings of the IEEE International Conference on Acoustics, Speech and Signal Processing*, Salt Lake City, USA, 2001.

[14] Rudolph van der Merwe, *Sigma-Point Kalman Filters for Probabilistic Inference in Dynamic State-Space Models*, Doctoral Thesis, OGI School of Science & Engineering at Oregon Health & Science University, USA, 2004.

[15] P. Zarchan and H. Musoff, *Fundamentals of Kalman Filtering: A Practical Approach*, AIAA, Second printing, 2000.